

Supporting Information

Hierarchical Layer-by-Layer Porous FeCo₂S₄@Ni(OH)₂ Arrays for All-Solid-State Asymmetric Supercapacitors

Shuo Li,^a Wei Huang,^b Yuan Yang,^a Jens Ulstrup,^b Lijie Ci,^a Jingdong Zhang,^b Jun Lou^{*c}, Pengchao Si^{*a}

^a SDU & Rice Joint Center for Carbon Nanomaterials, Key Laboratory for Liquid-Solid Structural Evolution and Processing of Materials, Ministry of Education, School of Materials Science and Engineering, Shandong University, Jinan 250061, P. R. China
E-mail: pcsi@sdu.edu.cn

^b Department of Chemistry, Technical University of Denmark, DK-2800 Kongens Lyngby, Denmark

^c SDU & Rice Joint Center for Carbon Nanomaterials, Department of Materials Science and NanoEngineering, Rice University, Houston, TX 77005, USA
E-mail: jlou@rice.edu

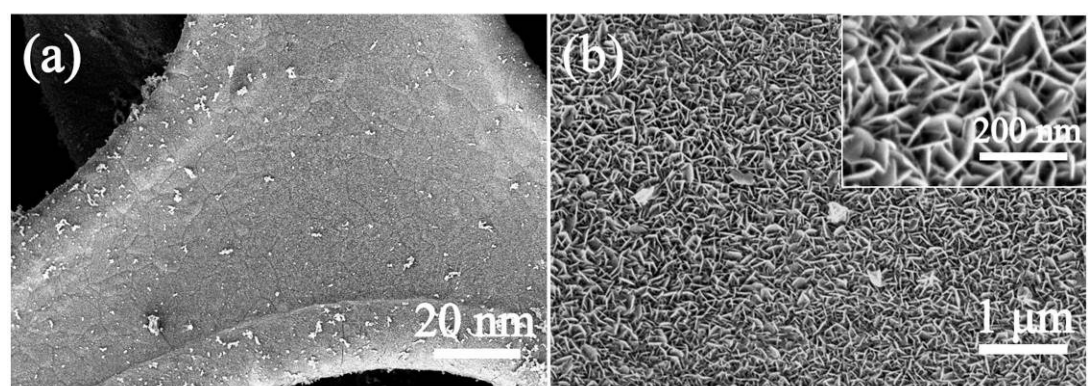


Fig. S1 a, b) SEM images of the Fe-Co precursors. The inset in b) shows the magnified Fe-Co precursor arrays.

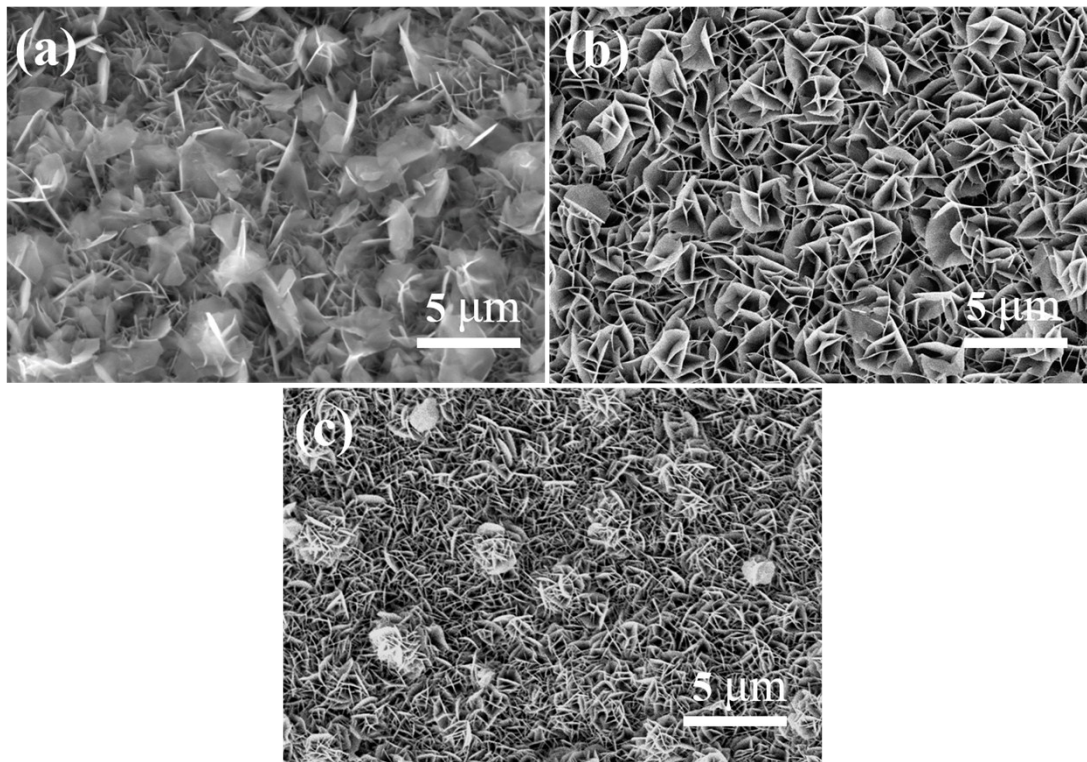


Fig. S2 SEM images of $\text{FeCo}_2\text{S}_4@\text{Ni}(\text{OH})_2$ layer-by-layer arrays with different $\text{Ni}(\text{OH})_2$ growth times: a) 3 h, b) 6 h, and c) 9 h.

For the sample $\text{FeCo}_2\text{S}_4@\text{Ni}(\text{OH})_2$ with $\text{Ni}(\text{OH})_2$ growth time of 3 h, Ni^{2+} reacted with OH^- to form nuclei and partially covered the Fe-Co precursors. The FeCo_2S_4 layer with smaller size under the $\text{Ni}(\text{OH})_2$ nanosheets can also be observed. With the growth time increasing to 6 h, the upper $\text{Ni}(\text{OH})_2$ nanosheets were distributed uniformly and formed organized arrays spontaneously which can provide adequate free space to ensure full contact between the two layers and the electrolyte. When further increasing the time to 9 h, the $\text{Ni}(\text{OH})_2$ nanosheets grew densely and even self-assembled into nanoflowers upon the $\text{Ni}(\text{OH})_2$ layer. This crowded distribution may prevent the effective transmission of the ions and reduce the utilization of the FeCo_2S_4 nanosheets.

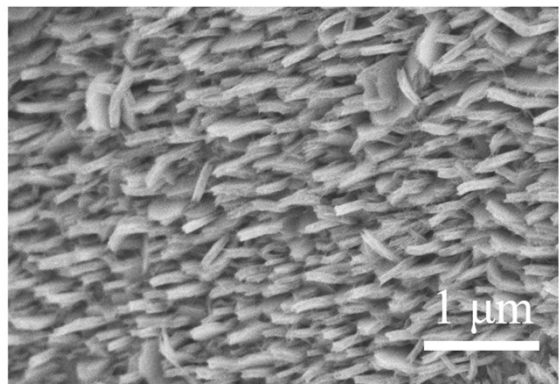


Fig. S3 SEM image of the solitary $\text{Ni}(\text{OH})_2$ nanosheets which were directly deposited on Ni foam.

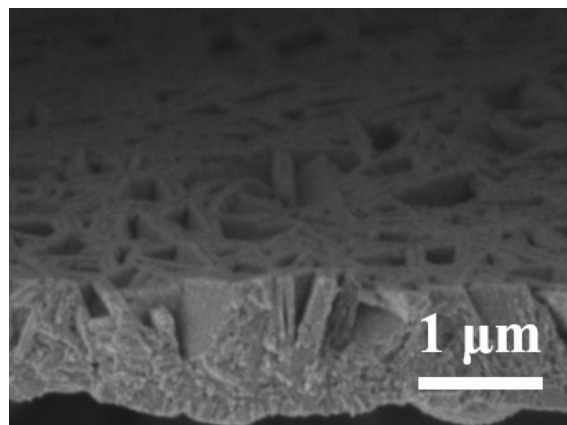


Fig. S4 SEM image of the cross section for the FeCo_2S_4 layer alone.

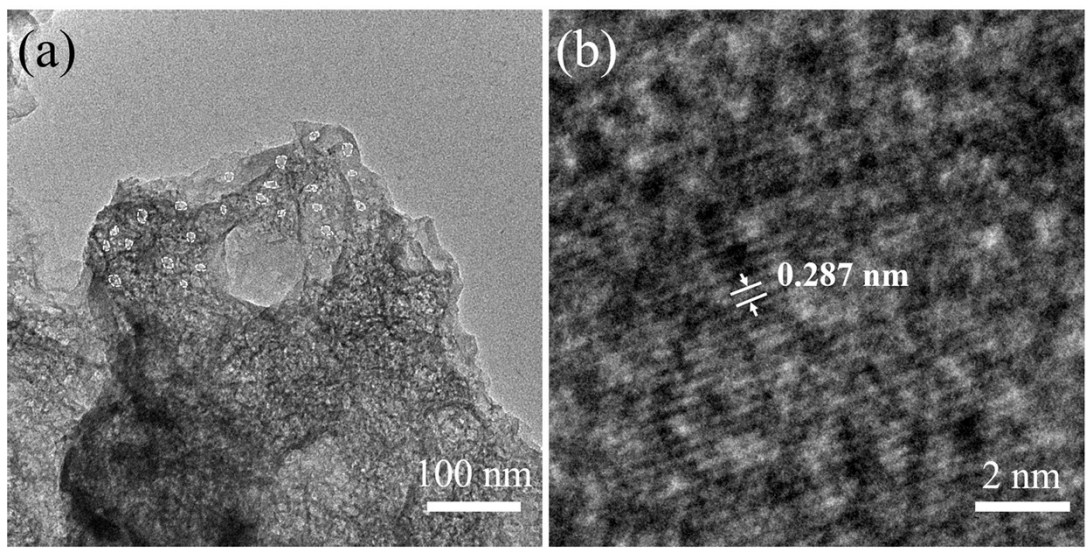


Fig. S5 a) TEM and b) HRTEM images of the FeCo_2S_4 nanosheet.

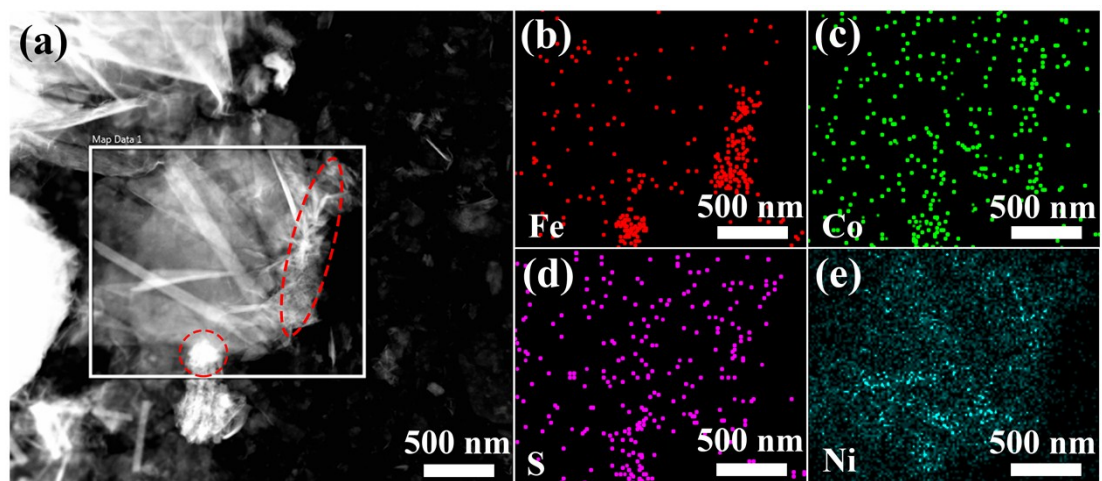


Fig. S6 a) STEM image of the $\text{FeCo}_2\text{S}_4@(\text{Ni(OH})_2$ hybrid nanosheets and the relevant STEM-EDS color elemental mapping of b) Fe-K, c) Co-K, d) S-K and e) Ni-K.

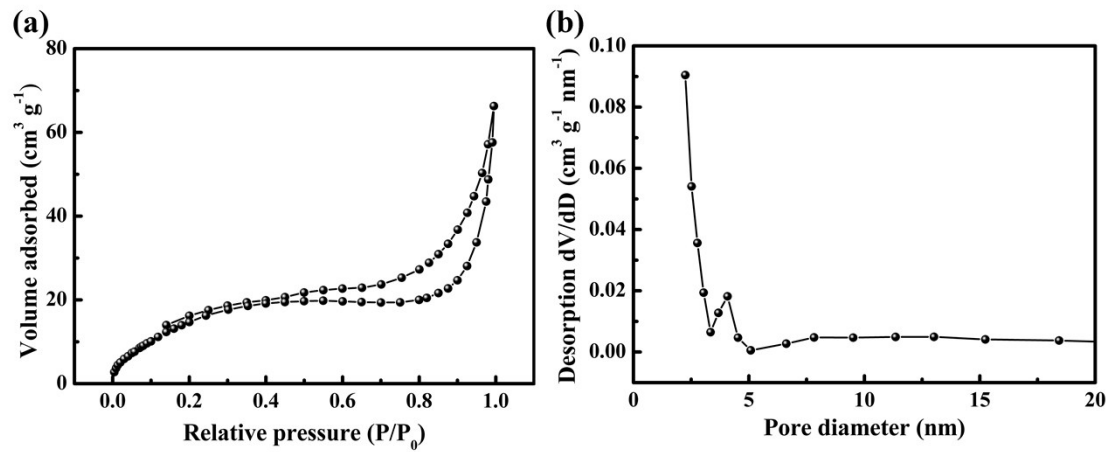


Fig. S7 a) N_2 adsorption and desorption isotherms of Ni(OH)_2 . b) Pore-size distribution of $\text{FeCo}_2\text{S}_4@\text{Ni(OH)}_2$.

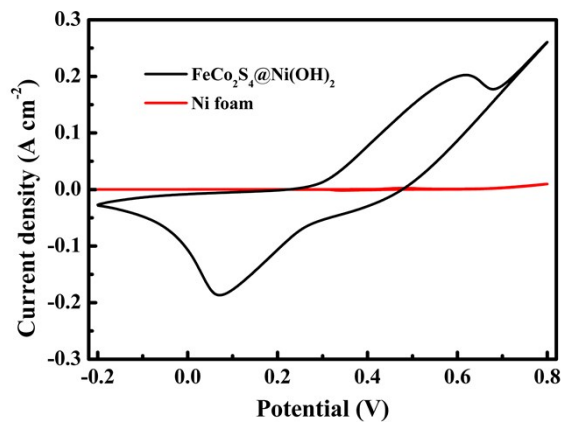


Fig. S8 CV curves of $\text{FeCo}_2\text{S}_4@\text{Ni(OH)}_2$ and pristine Ni foam electrodes at a scan rate of 20 mV s^{-1} .

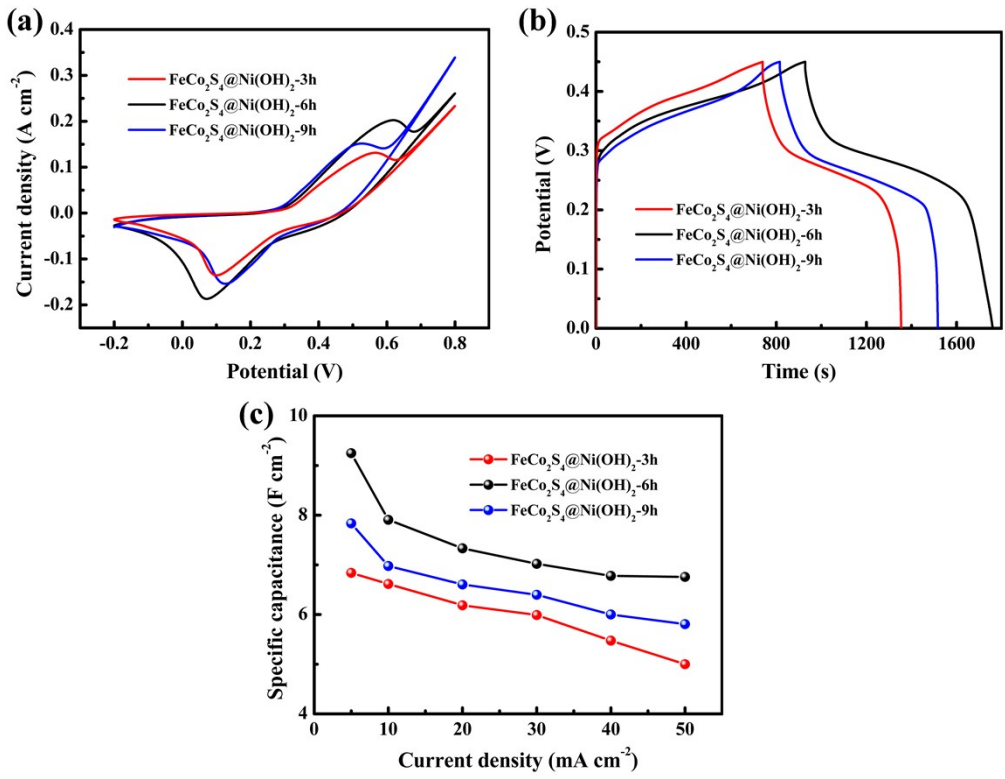


Fig. S9 a) CV curves of $\text{FeCo}_2\text{S}_4@\text{Ni(OH)}_2$ electrodes with different Ni(OH)_2 growth times (3, 6, and 9 h) at a scan rate of 20 mV s^{-1} . b) GCD curves of $\text{FeCo}_2\text{S}_4@\text{Ni(OH)}_2$ electrodes with different Ni(OH)_2 growth times (3, 6, and 9 h) at a current density of 5 mA cm^{-2} . c) Specific capacitance of $\text{FeCo}_2\text{S}_4@\text{Ni(OH)}_2$ electrodes with different Ni(OH)_2 growth times (3, 6, and 9 h) at various current densities.

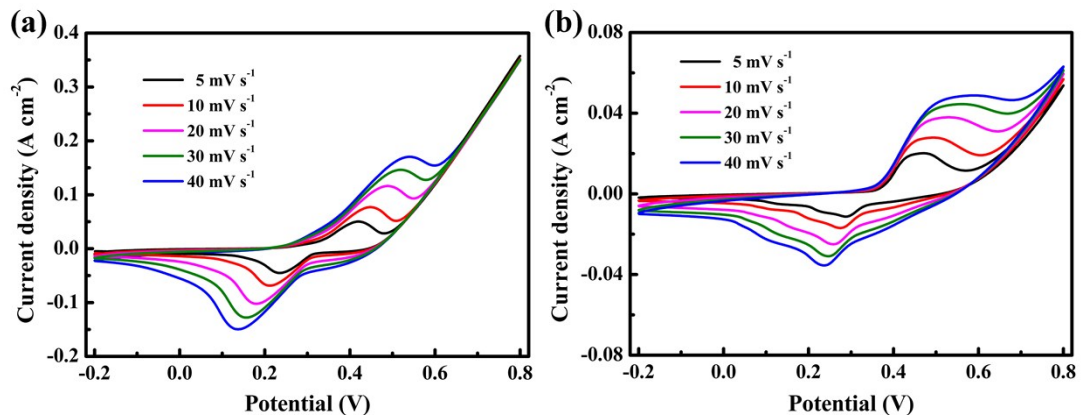


Fig. S10 CV curves of a) FeCo_2S_4 and b) Ni(OH)_2 electrodes at different scan rates.

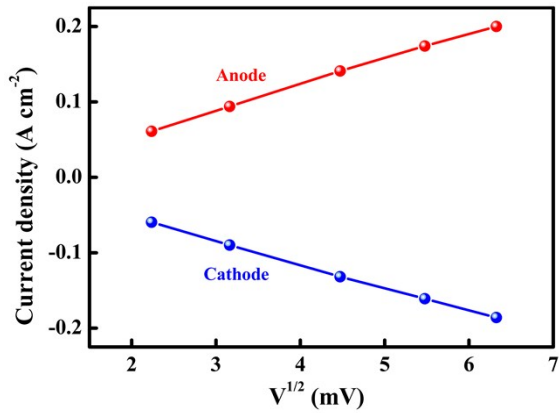


Fig. S11 Linear relationship between the anodic/cathodic peak currents and the square root of the scan rates.

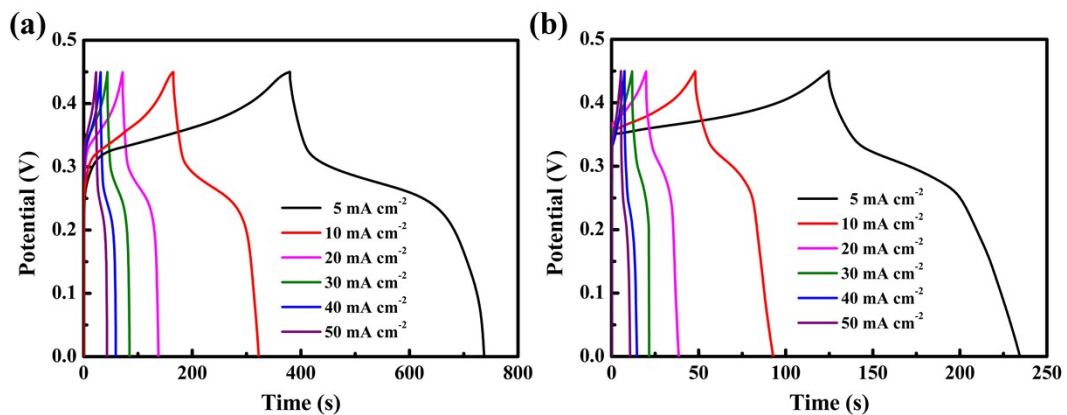


Fig. S12 GCD curves of c) FeCo_2S_4 and d) Ni(OH)_2 electrodes at different current densities.

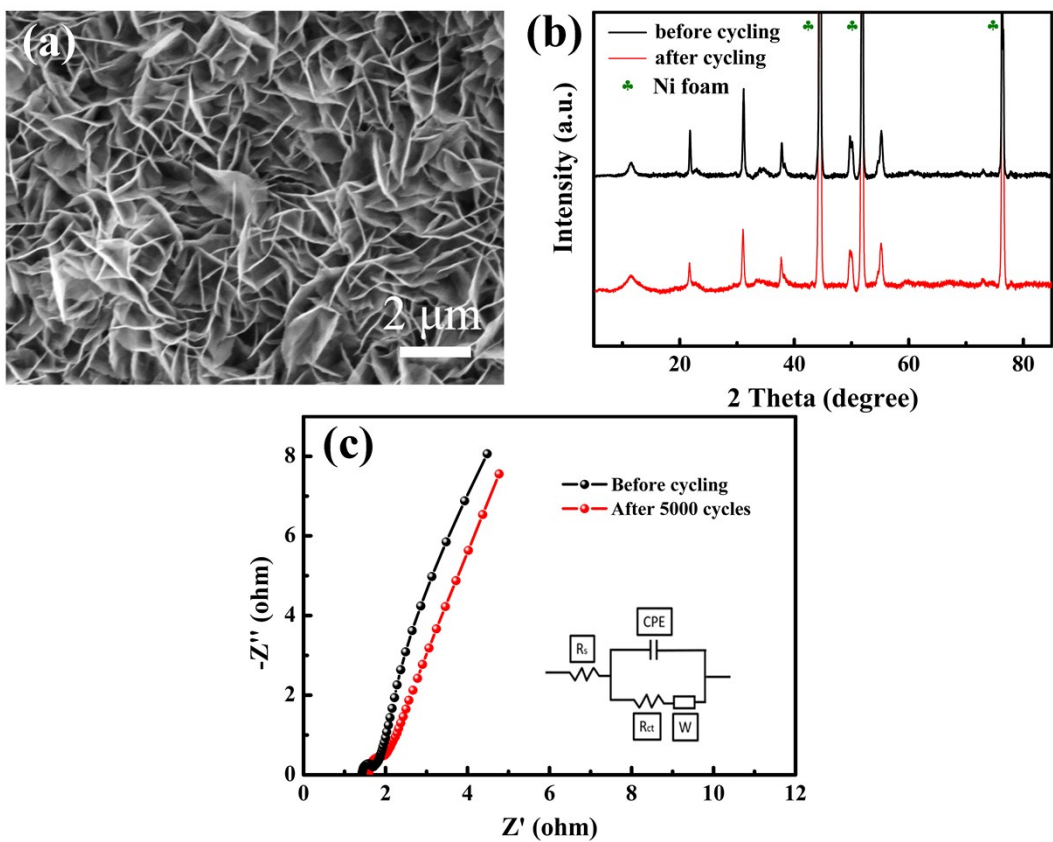


Fig. S13 a) Morphology of FeCo₂S₄@Ni(OH)₂ electrode after 5000 GCD cycles and the inset shows a magnified morphology. b) The XRD pattern of FeCo₂S₄@Ni(OH)₂ electrode after 5000 GCD cycles. c) EIS curves of FeCo₂S₄@Ni(OH)₂ electrode before and after 5000 GCD cycles. The inset shows the electrochemical equivalent circuit.

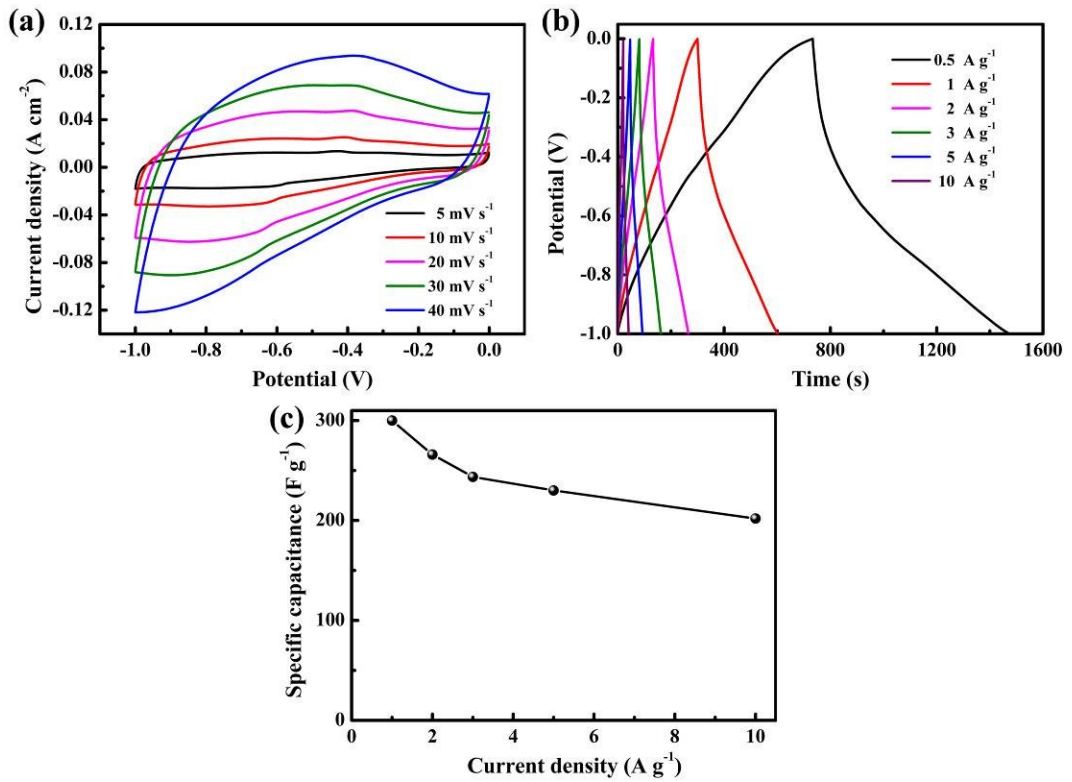


Fig. S14 a) CV curves of rGO electrode at different scan rates. b) GCD curves and c) specific capacitance of rGO electrode at different current densities.

Table S1. Comparison of electrochemical properties of FeCo₂S₄@Ni(OH)₂ nanosheet hybrid electrode with previous reports on related systems.

Electrode materials	Specific capacitance	Rate capability	Cycling stability	Ref.
FeCo ₂ S ₄ @Ni(OH) ₂ nanosheet hybrid	2984 F g ⁻¹ at 5 mA cm ⁻² (1.6 A g ⁻¹)	72% from 5 to 50 mA cm ⁻² (from 1.6 to 16 A g ⁻¹)	95.7% after 5000 cycles	This work
FeCo ₂ S ₄ micron tubes	2411 F g ⁻¹ at 5 mA cm ⁻² (1.7 A g ⁻¹)	72% from 5 to 40 mA cm ⁻² (from 1.7 to 13.3 A g ⁻¹)	93.4% after 3000 cycles	¹
FeCo ₂ S ₄ –NiCo ₂ S ₄ nanotubes	1519 F g ⁻¹ at 5 mA cm ⁻²	85.1% from 5 to 40 mA cm ⁻²	95.1% after 5000 cycles	²
Zn _{0.76} Co _{0.24} S nanotubes	2157 F g ⁻¹ at 1 A g ⁻¹	71% from 1 to 20 A g ⁻¹	78% after 10000 cycles	³
CoNi ₂ S ₄ arrays	2700 F g ⁻¹ at 5 mA cm ⁻² (4.76 A g ⁻¹)	69% from 4.76 to 47.6 A g ⁻¹	80.9% after 3000 cycles	⁴
NiCo ₂ S ₄ nanosheets	1231 F g ⁻¹ at 2 A g ⁻¹	71% from 2 to 20 A g ⁻¹	90.4% after 2000 cycles	⁵
Tube-like NiCo ₂ S ₄	1048 F g ⁻¹ at 3 A g ⁻¹	50% from 3 to 10 A g ⁻¹	75.9% after 5000 cycles	⁶
NiCo ₂ S ₄ hollow spheres	1036 F g ⁻¹ at 1 A g ⁻¹	68% from 1 to 20 A g ⁻¹	87% after 2000 cycles	⁷
NiCo ₂ S ₄ @Ni(OH) ₂	2700 F g ⁻¹ at 1 mA cm ⁻²	59% from 1 to 20 mA cm ⁻²	78% after 2000 cycles	⁸
MnCo-LDH@Ni(OH) ₂	2320 F g ⁻¹ at 3 A g ⁻¹	56% from 3 to 30 A g ⁻¹	90.9% after 5000 cycles	⁹

FeCo ₂ O ₄ @NiCo-LDH	2426 F g ⁻¹ at 1 A g ⁻¹	72.5% from 1 to 20 A g ⁻¹	91.6% after 5000 cycles	¹⁰
Co ₃ O ₄ @Ni(OH) ₂ nanosheets	1306 F g ⁻¹ at 1 mA cm ⁻²	46% from 1 to 12 A g ⁻¹	90% after 3000 cycles	¹¹
MnCo ₂ O ₄ @Ni(OH) ₂ Nanoflowers	2154 F g ⁻¹ at 5 mA cm ⁻²	33% from 5 to 20 A g ⁻¹	—	¹²

Table S2. Comparison of ASC device electrochemical performance with related systems reported.

ASC device	Energy density	Power density	Cycling stability	Ref.
FeCo ₂ S ₄ @Ni(OH) ₂ nanosheet//rGO	64 Wh kg ⁻¹	800 W kg ⁻¹	92.9% after 10000 cycles	This work
NiCo ₂ S ₄ //OMC (ordered mesoporous carbon)	45.5 Wh kg ⁻¹	512 W kg ⁻¹	70.4% after 10000 cycles	⁵
Ni-Co-S//PCNS (porous carbon nanosheets)	43.3 Wh kg ⁻¹	800 W kg ⁻¹	85% after 10000 cycles	¹³
NiCo ₂ S ₄ /Co ₉ S ₈ //AC	33.5 Wh kg ⁻¹	150 W kg ⁻¹	70% after 5000 cycles	¹⁴
Ni ₃ S ₂ /NiCo ₂ S ₄ //AC	40 Wh kg ⁻¹	1730 W kg ⁻¹	92.8% after 6000 cycles	¹⁵
NiCo ₂ S ₄ //rGO/Fe ₂ O ₃	61.7 Wh kg ⁻¹	1200 W kg ⁻¹	90% after 1000 cycles	¹⁶
Zn _{0.76} Co _{0.24} S//NGN/CNTs (nitrogen-doped graphene/carbon nanotubes)	50.2 Wh kg ⁻¹	387.5 W kg ⁻¹	100% after 2000 cycles	¹⁷
NiCo ₂ S ₄ @Co(OH) ₂ //AC	35.89 Wh kg ⁻¹	400 W kg ⁻¹	70% after 5000 cycles	¹⁸
CuCo ₂ S ₄ //rGO	50 Wh kg ⁻¹	700 W kg ⁻¹	78.2% after 5000 cycles	¹⁹
NiCo ₂ S ₄ //MWCNTs (multi-wall CNT)	51.8 Wh kg ⁻¹	865 W kg ⁻¹	85.7% after 5000 cycles	²⁰
NiCo ₂ S ₄ //AC	40.1 Wh kg ⁻¹	451 W kg ⁻¹	89.2% after 3000 cycles	²¹

Notes and references

1. S. Tang, B. Zhu, X. Shi, J. Wu and X. Meng, *Adv. Energy Mater.*, 2017, **7**, 1601985.
2. J. Zhu, S. Tang, J. Wu, X. Shi, B. Zhu and X. Meng, *Adv. Energy Mater.*, 2017, **7**, 1601234.
3. J. A. Syed, J. Ma, B. Zhu, S. Tang and X. Meng, *Adv. Energy Mater.*, 2017, **7**, 1701228.
4. L. Mei, T. Yang, C. Xu, M. Zhang, L. Chen, Q. Li and T. Wang, *Nano Energy*, 2014, **3**, 36-45.
5. L. Shen, J. Wang, G. Xu, H. Li, H. Dou and X. Zhang, *Adv. Energy Mater.*, 2015, **5**, 1400977.
6. Y. Zhang, M. Ma, J. Yang, C. Sun, H. Su, W. Huang and X. Dong, *Nanoscale*, 2014, **6**, 9824-9830.
7. L. Shen, L. Yu, H. B. Wu, X. -Y. Yu, X. Zhang and X. W. Lou, *Nat Commun*, 2015, **6**, 6694.
8. J. Zhang, H. Gao, M. Y. Zhang, Q. Yang and H. X. Chuo, *Appl Surf Sci*, 2015, **349**, 870-875.
9. S. Liu, S. C. Lee, U. Patil, I. Shackery, S. Kang, K. Zhang, J. H. Park, K. Y. Chung and S. C. Jun, *J. Mater. Chem. A*, 2017, **5**, 1043-1049.
10. X. He, R. Li, J. Liu, Q. Liu, R. R. chen, D. Song and J. Wang, *Chem Eng J*, 2018, **334**, 1573-1583.
11. X. Bai, Q. Liu, J. Liu, H. Zhang, Z. Li, X. Jing, P. Liu, J. Wang and R. Li, *Chem Eng J*, 2017, **315**, 35-45.
12. Y. Zhao, L. Hu, S. Zhao and L. Wu, *Adv. Funct. Mater.*, 2016, **26**, 4085-4093.
13. J. Yang, C. Yu, X. Fan, S. Liang, S. Li, H. Huang, Z. Ling, C. Hao and J. Qiu, *Energ. Environ. Sci.*, 2016, **9**, 1299-1307.
14. L. Hou, Y. Shi, S. Zhu, M. Rehan, G. Pang, X. Zhang and C. Yuan, *J. Mater. Chem. A*, 2017, **5**, 133-144.
15. W. He, C. Wang, H. Li, X. Deng, X. Xu and T. Zhai, *Adv. Energy Mater.*, 2017, **7**, 1700983.
16. Y. Wang, Z. Chen, T. Lei, Y. Ai, Z. Peng, X. Yan, H. Li, J. Zhang, Z. M. Wang and Y. -L. Chueh, *Adv. Energy Mater.*, 2018, **8**, 1870076.
17. H. Tong, W. Bai, S. Yue, Z. Gao, L. Lu, L. Shen, S. Dong, J. Zhu, J. He and X. Zhang, *J. Mater. Chem. A*, 2016, **4**, 11256-11263.
18. R. Li, S. Wang, Z. Huang, F. Lu and T. He, *J. Power Sources*, 2016, **312**, 156-164.
19. X. Yuan, B. Tang, Y. Sui, S. Huang, J. Qi, Y. Pu, F. Wei, Y. He, Q. Meng and P. Cao, *J. Mater. Sci-Mater. El.*, 2018, **29**, 8636-8648.
20. P. Wen, M. Fan, D. Yang, Y. Wang, H. Cheng and J. Wang, *J. Power Sources*, 2016, **320**, 28-36.
21. L. Hao, L. Shen, J. Wang, Y. Xu and X. Zhang, *Rsc Advances*, 2016, **6**, 9950-9957.